

# Phase Contrast and Surface Energy Hysteresis in Tapping Mode Scanning Force Microscopy

Ricardo García,\* Javier Tamayo and Alvaro San Paulo

Instituto de Microelectrónica de Madrid, CSIC, Isaac Newton 8, 28760 Tres Cantos, Madrid, Spain

Phase imaging is one of the most attractive features of tapping mode scanning force microscopy operation. In this paper we analyse the relationship between phase contrast imaging and the energy loss due to tip-sample interaction forces. An analytical relationship is obtained between the phase shift and the energy loss. Experiments performed on graphite are in agreement with the analytical expression. Copyright © 1999 John Wiley & Sons, Ltd.

KEYWORDS: AFM; phase imaging; friction

## INTRODUCTION

The tapping mode operation of a scanning force microscope is widely used to image samples in air or under liquids.<sup>1–6</sup> In the imaging mode, the cantilever tip ensemble is oscillated at a frequency close to its free resonance frequency (usually in the 100–300 kHz range) while the feedback mechanism keeps the oscillation amplitude ( $A_t$ , called the set point amplitude) at a constant value. It is assumed that the equilibrium tip-sample separation is smaller than the oscillation amplitude and as a consequence the tip strikes the sample once each cycle. Large amplitudes (up to 100 nm) and rigid cantilevers (about  $20 \text{ N m}^{-1}$ ) are thought to be needed for providing the cantilever with enough energy to overcome adhesion forces. The substantial reduction of the lateral force exerted on the sample, in comparison with contact scanning force microscopy (SFM), explains its ability to image very compliant materials.<sup>4</sup> It has also been proposed that the difference in phase angles between the excitation signal and the deflection of the cantilever (phase shift) could be sensitive to compositional variations in heterogeneous samples.<sup>4–5,7–8</sup> Imaging phase shift changes (phase contrast images or phase imaging) is a rich and powerful tool for enhancing sharp topographic changes in rough surfaces as well as for imaging heterogeneous samples. However, in spite of its wide experimental use, several key issues of tapping operation, such as how to interpret height and phase contrast images in terms of the sample properties, are still open.

In this paper we study the influence of tip-sample elastic and inelastic interactions on phase shifts. The cantilever dynamics in tapping operation are described by a non-linear model. It is deduced that in the absence of inelastic interactions, phase shifts are independent of the value of the elastic modulus. However, phase shifts

associated with elastic property variations arise if a fraction of the cantilever's kinetic energy is dissipated by the tip-sample interaction forces. More generally, it is also demonstrated that the sine of the phase shift is proportional to the energy dissipated by the tip-sample interaction forces.

## MODEL

Several approaches have been proposed to describe the tapping mode operation.<sup>4,9–14</sup> Here, it is assumed that the cantilever behaviour can be simulated by a non-linear driven oscillator with damping. Then, the movement of the cantilever is governed by

$$m \frac{dz^2}{dt^2} = -k_c z - \frac{mw_0}{Q} \frac{dz}{dt} + F_{ts} + F_0 \cos \omega t \quad (1)$$

where  $k_c$ ,  $\omega_0 = 2\pi f_0$  and  $Q$  are the elastic constant, resonance frequency and quality factor of the cantilever, respectively, the sinusoidal term is the excitation signal applied to the cantilever, where  $\omega$  is the excitation (tapping) frequency; and  $F_{ts}(z_c, z)$  is the tip-sample interaction, where  $z_c$  is the equilibrium tip-sample separation and  $z$  is the tip's instantaneous position.

During an oscillation, the cantilever goes through non-contact and contact tip sample conditions. These situations are separated by the interatomic distance  $a_0$ . For distances larger than  $a_0$  the tip-sample interaction is calculated through the van der Waals force between a sphere and a flat surface. For distances smaller than  $a_0$ , the repulsive force is simulated by the indentation force between a paraboloid (tip) and a flat (sample) derived from Hertz's model (see Ref. 4 for details).

The adhesion force when the tip approaches the sample is the value of the van der Waals force at the interatomic distance. The surface energy is estimated by using the adhesion force given by the Johnson-Kendall-Roberts (JKR) model

$$F_a = -3\pi R\gamma_x \quad (2)$$

\* Correspondence to: R. García, Instituto de Microelectrónica de Madrid, CSIC, Isaac Newton 8, 28760 Tres Cantos, Madrid, Spain.  
E-mail: rgarcia@imm.cnm.csig.es

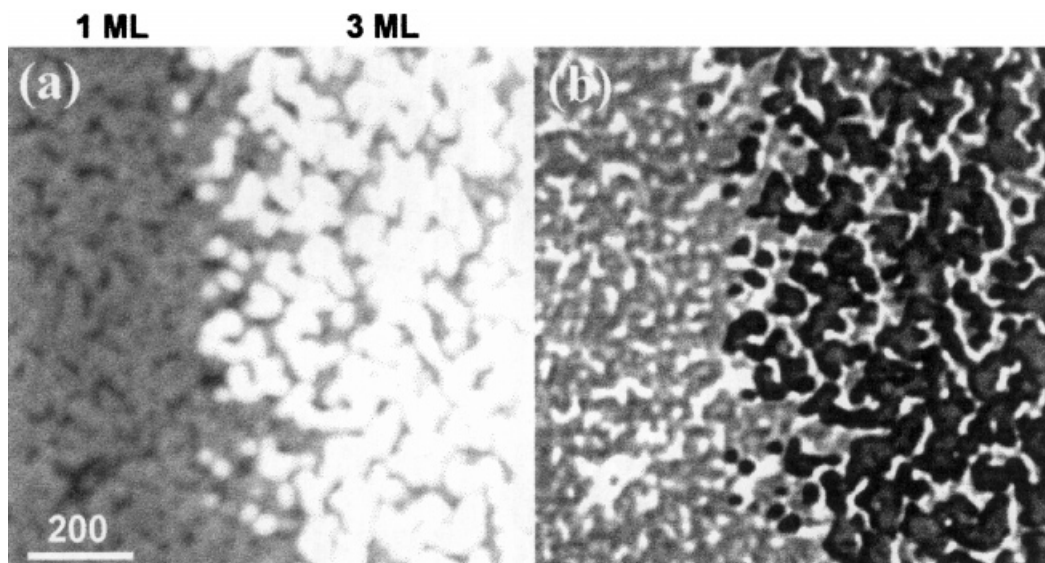


**Figure 1.** Tapping mode SFM images of a Langmuir–Blodgett film interface on Si(100): (a) topography; (b) phase contrast image of the 1 ML/3 ML interface. The morphological details are more clearly imaged in the phase image than in the topography. Parameters:  $A_0 = 25$  nm;  $A_t/A_0 = 0.63$ ;  $f = f_0 = 322$  kHz.

where  $\gamma_x$  is the tip–sample surface energy during approach ( $x = A$ ) or retraction ( $x = R$ ).

In this paper, a channel for inelastic tip–sample interactions is opened when surface energy hysteresis is considered ( $\gamma_a \neq \gamma_R$ ).<sup>15,16</sup>

#### PHASE CONTRAST IMAGE IN A LANGMUIR–BLODGETT FILM

An example of the potential of phase contrast imaging to characterize the morphology of Langmuir–Blodgett films and heterogeneous samples is shown in Fig. 1. The sample was prepared by deposition of a monolayer (ML) of an amphiphilic dendrimer on the substrate, Si(100). Then, two more monolayers were selectively deposited on the first monolayer. Figure 1 shows the topographic image [Fig. 1(a)] and the phase shift image [Fig. 1(b)] of the 1 ML/3 ML interface. Due to the differences in height (the first and the third monolayer have an average height of  $\sim 2$  and  $\sim 5$  nm, respectively), it is more tedious to extract detailed morphological information from the topographic image. The phase shift image, on the other hand, reveals clearly 1 ML and 3 ML domains. In the 1 ML layer region, the white spots (higher phase shift) correspond to regions of the silicon substrate that were not covered by the film.

#### PHASE SHIFT DEPENDENCE ON YOUNG'S MODULUS AND SURFACE ENERGY HYSTERESIS

Phase contrast images obtained in heterogeneous samples by tapping mode SFM, i.e., at constant oscillation amplitude, have been linked directly to variations of elastic properties.<sup>17</sup> Although variations in the Young's modulus of the sample could give rise to phase shift changes, we show below that there is not a direct

relationship between them. In earlier contributions, it has been demonstrated that the essential feature dominating phase shifts is the existence of tip–sample inelastic interactions.<sup>14,18</sup> This is illustrated in the simulation shown in Fig. 2, where the phase shift is calculated as a function of Young's modulus. The simulation is performed by assuming an amplitude ratio  $A_t/A_0$  of 0.6, where  $A_0$  is the free oscillation amplitude. When the tip–sample interaction involves exclusively elastic processes (circles), the phase shift is independent of the sample's Young's modulus  $E$  variations over a range of four orders of magnitude.

The introduction of hysteresis in the surface energy (adhesion energy hysteresis) modifies the phase shift behaviour considerably. The phase shift is very sensitive

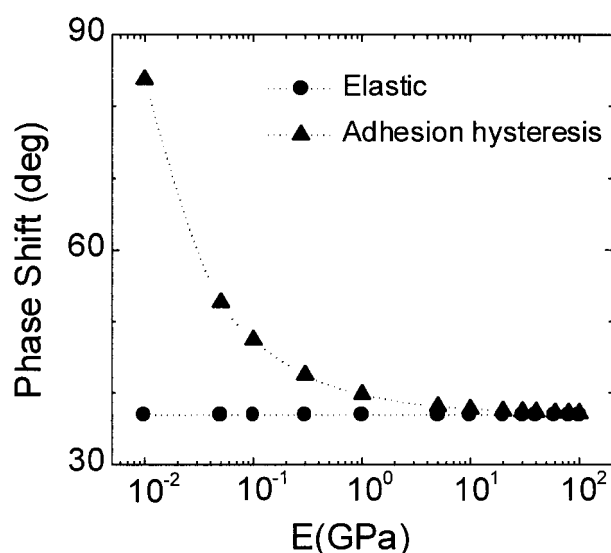


**Figure 2.** Theoretical phase shift dependence on Young's modulus for several tip–sample interactions: elastic interactions (open circles); for a tip–sample interaction with adhesion energy hysteresis,  $\gamma_A = 10$  mJ m<sup>-2</sup> and  $\gamma_R = 60$  mJ m<sup>-2</sup> (triangles);  $A_t/A_0 = 0.6$ ,  $Q = 500$ ,  $k_c = 20$  N m<sup>-1</sup> and  $f = 200$  KHz.

to changes in the elasticity of compliant materials, e.g., materials with Young's modulus below 1 GPa. The phase shift decreases with the stiffness of the sample, being almost constant for stiff materials. This value (36.8° here) is set by the initial tapping conditions ( $A_t/A_0$  and  $f/f_0$ ). A similar dependence has been found when the sample's viscoelasticity was introduced in the model.<sup>14</sup>

The independence of the phase shift with the Young modulus in the absence of inelastic interactions appears to be counter-intuitive. An explanation for this behaviour is provided in the next section.

### ANALYTICAL RELATIONSHIP BETWEEN THE PHASE SHIFT AND THE TIP-SAMPLE ENERGY DISSIPATION

A relationship between the phase shift and the energy dissipated in tapping mode SFM is obtained by considering that in the steady state the external energy ( $E_{\text{ext}}$ ) supplied to the cantilever must equal the energy dissipated via hydrodynamic viscous interactions with the environment (air) and by the tip-sample inelastic interactions<sup>19,20</sup>

$$E_{\text{ext}} = E_{\text{air}} + E_{\text{dis}} \quad (3)$$

where

$$E_{\text{ext}} = \oint F_0 \cos \omega t \frac{dz}{dt} dt \quad (4)$$

$$E_{\text{air}} = \oint -\frac{m\omega_0}{Q} \frac{dz}{dt} dz \quad (5)$$

$$E_{\text{dis}} = \oint F_{\text{ts}} \frac{dz}{dt} dt \quad (6)$$

The above equations and the assumptions of a sinusoidal cantilever response provide an expression that relates the phase shift angle ( $\varphi$ ) to the energy dissipated by the tip-sample interactions  $E_{\text{dis}}$  per period

$$\sin \varphi = \frac{\omega}{\omega_0} \frac{A_t(\omega)}{A_0} + \frac{QE_{\text{dis}}}{\pi k A_0 A_t(\omega)} \quad (7)$$

where  $\omega$  and  $\omega_0$  are the excitation and natural frequencies of the cantilever, respectively;  $A_t(\omega)/A_0$  ( $\omega$ ) represents the contribution due to elastic effects while  $QE_{\text{dis}}/\pi k A_0 A_t$  represents the inelastic contributions.

To check the validity of the above equation, an experiment was designed to measure the phase shift dependence on the tapping amplitude<sup>20</sup>. The experiment was performed on a graphite (HOPG) surface with a free amplitude of  $A_0 = 43$  nm. The cantilever was excited at its resonance frequency. For all the  $A_t$  values used there is tip-sample contact at the sample end of the oscillation. To check for homogeneity of the data, the experiment has been repeated on 64 different spots of the sample. No differences were obtained. The experimental data were derived from the phase shift and amplitude versus equilibrium tip-sample separation curves taken simultaneously (not shown).

In Fig. 3 the continuous line represents the theoretical simulation obtained from Eqn. (7), with  $E_{\text{dis}}$  as the only fitting parameter. It is remarkable that there is

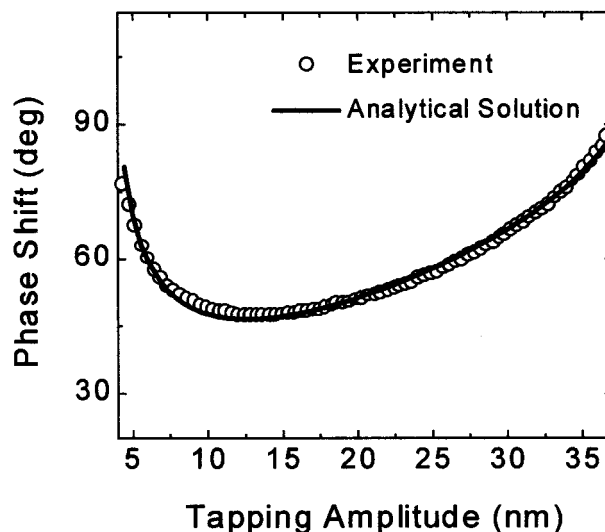


**Figure 3.** Phase shift dependence on the tapping amplitude for the graphite (circles). The solid line is the result obtained from Eqn. (7). Instrumental data:  $f/f_0 = 1$ ,  $A_0 = 43$  nm,  $k = 45$  N m<sup>-1</sup> and  $Q = 270$ .

numerical as well as shape agreement between the experimental and simulated data over the  $A_t$  range explored. The fitting was achieved with  $E_{\text{dis}} = 510$  eV. For  $A_t$  amplitudes between 35 nm and 10 nm ( $A_0 = 43$  nm) the phase shift decreases. In this region the  $A/A_0$  ratio is the dominant factor in the phase shift. However, for smaller  $A_t$  values the second term becomes dominant and the phase shift increases.

To exclude a fortuitous agreement, another experiment was performed to measure directly the energy dissipated by the tip-sample forces. The force was recorded while the cantilever was approached and then retracted from the sample, i.e. a force curve was taken. From the hysteresis loop shown in the force curves,  $E_{\text{ts}} = 480$  eV is deduced. The agreement obtained between the measured and simulated data supports the conclusions derived from the relationship between the phase shift and the energy loss established in Eqn. (7). A similar experiment was performed on a soft material (purple membrane) with identical conclusions.

In tapping mode SFM imaging the oscillation amplitude is kept constant ( $A_t = \text{constant}$ ) so that the first term of Eqn. (7) does not change with location of the sample. If phase shifts are observed in the image they should arise from  $E_{\text{dis}}$  variations, as the simulation in Fig. 2 has shown.

### COMPARISON BETWEEN FRICTION FORCE AND PHASE SHIFT IMAGES

Friction force microscopy (FFM) has been applied as a tool to extract quantitative information about the chemical composition of heterogeneous samples.<sup>22,23</sup> In previous experiments we have applied FFM to characterize compositional variations in semiconductor heterostructures and quantum dots. Because friction is closely related to energy dissipation during the tip displacement across the sample, we have imaged a III-V semiconductor interface by FFM and tapping mode

SFM to investigate whether the relationship obtained between the phase shift and the energy dissipation is consistent with frictional force experiments.

Figures 4(a) and 4(b) show the topography and phase contrast images of an InP/InSb interface. The topography shows several terraces and steps but there is no information regarding the position of the interface's boundary. The phase image, on the other hand, clearly separates two regions of different and uniform phase shift. A higher phase shift is obtained in the InP (left side), implying that the tip-sample interaction dissipates more energy in the InP than in the InSb side.

Figures 4(c) and 4(d) show the topography and friction force images of the same InP/InSb interface but in a different region. A higher frictional force is obtained in the InP region of the interface (left) [Fig. 4(d)], implying a higher value for the energy loss. This result is consistent with the phase shift image of the same interface. Both techniques (FFM and tapping mode SFM) point out that InP is the region where more energy is dissipated by the tip-sample forces. Although it is suggestive, we do not imply that the mechanisms of energy dissipation on a nanometre scale by FFM and tapping mode SFM in semiconductor samples are the same.

---

## CONCLUSION

---

The effect of elastic and inelastic interactions (surface energy hysteresis) on phase shifts during tapping operation has been studied. In the absence of tip-sample inelastic interactions, phase shifts are insensitive to elastic modulus variations. Phase contrast images associated with elastic variations are obtained once a fraction of the kinetic energy is dissipated into the sample. A relationship between the phase shift and the energy loss at the tip-sample interface has been verified experimentally for tapping amplitudes larger than the equilibrium tip-sample separation. This relationship establishes a proportionality between the sine of the phase and the energy loss.

## Acknowledgements

We are very grateful to C. Elissen-Roman and Professor A. Meijer for providing the Langmuir-Blodgett films. This work has been supported by the European Commission (BICEPS, BIO4-CT97-2112).

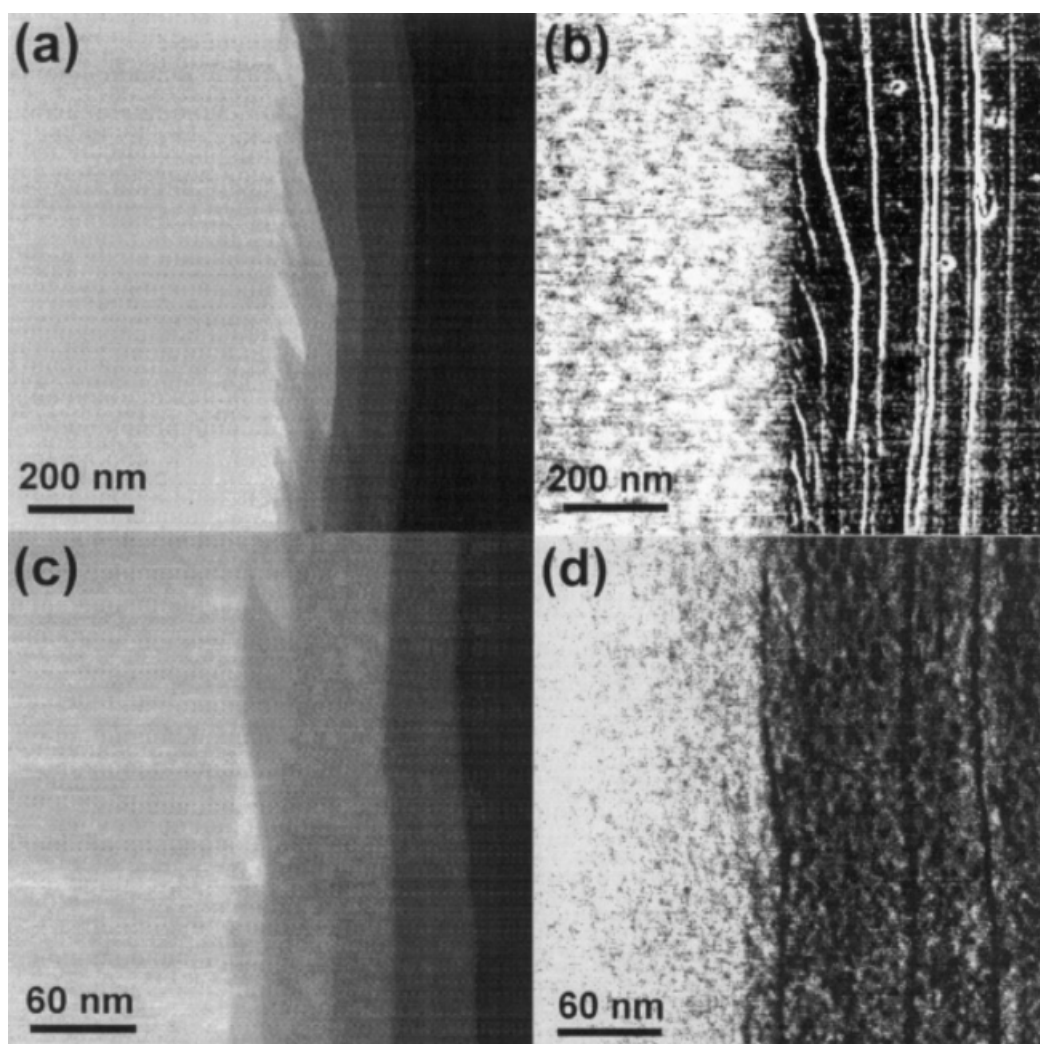


**Figure 4.** Tapping mode SFM and FFM images of an InP/InSb interface: (a) topography in tapping mode; (b) phase shift in tapping mode; (c) topography of FFM image; (d) frictional force image in contact SFM.

## REFERENCES

1. Q. Zhong, D. Imniss, K. Kjoller and V. B. Elings, *Surf. Sci.* **290**, L688 (1993).
2. C. Putman, K. Van der Werf, B. De Grooth, N. Van Hulst and J. Greve, *Appl. Phys. Lett.* **64**, 2454 (1994).
3. P. Hausma, J. P. Cleveland, M. Radmacher, D. A. Walters, P. E. Hillner, M. Bezanilla, M. Fritz, D. Vie, H. G. Hansma, C. B. Prater, J. Massie, L. Fukunaga, J. Gurley and V. Elings, *Appl. Phys. Lett.* **64**, 1738 (1994).
4. J. Tamayo and R. Garcia, *Langmuir* **12**, 4430 (1996).
5. T. Pompe, A. Fery and S. Herminhaus, *Langmuir* **14**, 2585 (1998).
6. K. Sasaki, Y. Koike, H. Azehara, H. Horaki and M. Fujihira, *Appl. Phys. A* **66**, 1275 (1998).
7. D. A. Chernoff, *Proceedings of Microscopy and Microanalysis 1995* Jones and Begell, New York (1995).
8. G. Bar, Y. Thomann, and M.-H. Whangbo, *Langmuir* **14**, 1219 (1998).
9. J. Chen, R. K. Workman, D. Sarid and R. Höper, *Nanotechnology* **5**, 199 (1994); D. Sarid, T. G. Russel, R. K. Workman and D. Chen, *J. Vac. Sci. Technol. B* **14**, 864 (1996).
10. B. Anczykowski, D. Krüger and H. Fuchs, *Phys. Rev. B* **53**, 15485 (1996).
11. R. G. Winkler, J. P. Spatz, S. Sheiko, M. Möller, R. Reineker and O. Marti, *Phys. Rev. B* **54**, 8908 (1996).
12. N. A. Burnham, O. P. Behrend, F. Oulevey, G. Gremaud, P.-J. Gallo, D. Gourdon, E. Dupas, A. J. Kulik, H. M. Pollock and G. A. D. Briggs, *Nanotechnology* **8**, 67 (1997).
13. A. Kühle, A. H. Soerensen and J. Bohr, *J. Appl. Phys.* **81**, 6562 (1997).
14. J. Tamayo and R. Garcia, *Appl. Phys. Lett.* **71**, 2394 (1997).
15. H. Yoshizawa, Y.-L. Chen and J. Israelachvili, *J. Phys. Chem.* **97**, 4128 (1993).
16. M. K. Chaudhury, *Mat. Sci. Eng.* **R16**, 97.159 (1996).
17. S. N. Magonov, V. Elings and M.-H. Whangbo, *Surf. Sci.* **375**, L385 (1997).
18. R. Garcia, J. Tamayo, M. Calleja and F. Garcia, *Appl. Phys. A* **66**, 309 (1998).
19. J. P. Cleveland, B. Anczykowski, A. E. Schmid and V. Elings, *Appl. Phys. Lett.* **72**, 2613 (1998).
20. J. Tamayo and R. Garcia, *Appl. Phys. Lett.* **73**, 2926 (1998).
21. N. A. Burham, R. J. Colton and H. Pollock, *Nanotechnology* **4**, 64 (1993).
22. E. Meyer, R. Lüthi, L. Howald, M. Bamberlin, M. Guggisberg, H.-J. Gütherodt, L. Scandella, J. Gobrecht, A. Schumaker, R. Prins, B. N. J. Persson and E. Tosatti (eds), *Physics of Sliding Friction 349*. Kluwer Academic, Dordrecht (1996).
23. J. Tamayo, L. González and R. Garcia, *Appl. Phys. Lett.* **68**, 2297 (1996).